Renewable Energy 121 (2018) 153–163

Contents lists available at ScienceDirect

Renewable Energy

journal homepage: www.elsevier.com/locate/renene

Development of the direct solar photocatalytic water splitting system for hydrogen production in Northwest China: Design and evaluation of photoreactor

Fei Cao [a, b, c, *], Qingyu Wei [b], Huan Liu [b], Na Lu [c], Liang Zhao [b, **], Liejin Guo [b]

[a] College of Mechanical and Electrical Engineering, Hohai University, Changzhou 213022, China
[b] State Key Laboratory of Multiphase Flow in Powering Engineering, Xi'an Jiaotong University, Xi'an 710049, China
[c] Lyles School of Civil Engineering, School of Materials Engineering, Birck Nanotechnology Center, Purdue University, West Lafayette, IN 47906, USA

ARTICLE INFO

Article history:
Received 14 January 2017
Received in revised form
20 December 2017
Accepted 5 January 2018

Keywords:
CPC reactor
Solar photocatalytic hydrogen production
Solar photocatalysis
Hydrogen production
Solar energy

ABSTRACT

A novel CPC reactor for solar photocatalytic hydrogen production was designed and evaluated in the present study. Two operation models, namely the natural circulation model and the gas disturbance model, are proposed and illustrated from the viewpoints of thermodynamics and hydrodynamics. The designed photoreactor is operated under natural circulation for most of the time, with high pressure gas disturbing the sedimentary photocatalysts from time to time. The CPC parameters are designed according to the local meteorological conditions. The reactor performance such as the radiation distribution on the absorber tube, the absorbed solar irradiation, the critical flow rates and the hydrogen productivity are estimated and analyzed. An east-west orientated, north-south angle adjustable and truncated CPC with the concentration ratio of 4.12 is designed for the photoreactor. The required limiting settling velocity is much larger than the natural circulation velocity, which validates the necessity of gas disturbance. The estimated results show that the ideal mean hydrogen productivities are 2.9 L/h and 4.0 L/h in a typical spring and summer week respectively, with the photocatalyst being $Cd_{0.5}Zn_{0.5}S$.

1. Introduction

Conventional energy resources such as coal and petroleum products have been depleted to a great extent. It is therefore necessary to produce an alternative fuel that should in principle be pollution free, storable and economical. Hydrogen satisfies the first two conditions and is expected to fulfill the third requirement. Photocatalytic hydrogen production from water using solar energy has been identified as a promising technology for the final realization of renewable hydrogen production. However, many problems must be addressed before this technology becomes economically viable. One issue is the development of efficient visible light driven photocatalyst which has undergone a rapid progress over the past years [1–3]. Another key issue concerns the efficient utilization of the solar energy itself. The design of the photocatalytic reactor is closely related to this aspect. Many different photocatalytic reactors have been developed, such as parabolic-trough concentrator (PTC) [4], thin-film-fixed-bed reactor (TFFBR) [5], double skin sheet reactor (DSSR) [6] and compound parabolic concentrator (CPC) [7–11]. The CPCs are frequently researched based on its great advantages that the concentrator geometry allows indirect light to be reflected onto the absorber tube, not needing sun-tracking and that it is of high cost-effectiveness [7–9]. Therefore it is an optimized option for solar photochemical applications [10,11]. On achieving the high efficiency photocatalysts and photoreactors, an important step forward is to combine them together for demonstrating the photocatalysis feasibility at pilot scales. One of the earliest pilot-scale constructions of CPC photoreactors was installed at the Plataforma Solar de Almeria (PSA), Spain for the purpose of water detoxification, whose collection area is 8.9 m^2 [7]. A scaling up of this pilot plant was then further developed for the batch treatment of 2 m^3 of water with a 100 m^2 collector area and aqueous aerated suspensions of polycrystalline TiO_2 [8]. Another low-cost CPC reactor were installed for the purpose of the destruction of 500 μg/L of selected pesticides to maximum permitted levels (0.1 μg/L) at the

* Corresponding author. College of Mechanical and Electrical Engineering, Hohai University, Changzhou 213022, China.
** Corresponding author.
E-mail addresses: fcao@hhu.edu.cn, yq.cao@hotmail.com (F. Cao), lzhao@mail.xjtu.edu.cn (L. Zhao).

https://doi.org/10.1016/j.renene.2018.01.016
0960-1481/

Institutode Maquina Herramienta [9].

The above mentioned pilot demonstrations were designed for photocatalytic detoxification or biological purposes. Some efforts have been carried out on the pilot demonstration of photocatalytic hydrogen production at the State Key Laboratory of Multiphase Flow in Power Engineering (SKLMFPE). Two generations of reactors have been developed for the photocatalytic hydrogen production, whose photos and major parameters are shown in Fig. 1 and Table 1 respectively [10,11].

The first generation is a closed indoor photocatalytic hydrogen production reactor irradiated by Xe lamp [10]. The second generation is an outdoor photoreactor with truncated CPCs and adjustable half acceptance angles [11]. It is the first time that direct solar photocatalytic water splitting for hydrogen production was realized in outdoor application. Its hydrogen production rate (0.164 L/h per unit volume of reaction solution) was observed to be larger than that of the lab-scale result (0.126 L/h). These photoreactors validated the feasibility of outdoor photocatalytic hydrogen production in CPC photoreactors. Their hydrogen production rates indicated a promising future for the direct solar, low-cost and mass solar hydrogen production [11]. However, from the commercial application point of view, these reactors were still constructed and operated in small scale. Moreover, no operation strategy is proposed for the photocatalytic hydrogen production process. In addition, the formal reactors were all circled by pumped and operated under forced circulation. It would be more cost-saving if the usage of pump is avoided or in less frequency. Based on these considerations, a new reactor is designed for pilot demonstration of the direct solar photocatalytic hydrogen production technology. The reactor is operated under natural circulation for most of the time, and the high pressure gas is filled to perturb the sedimentary photocatalysts from time to time. The CPC is designed according to meteorological conditions of the SKLMFPE. The reactor performances such as the radiation distribution on the absorber tube, the absorbed solar irradiation, the critical flow rates and the hydrogen productivity are estimated and analyzed.

2. System development

2.1. CPC design

Marginal lights of full-shape and truncated CPCs are shown in Fig. 2. Purpose of CPC's truncation is to reduce its material cost, configuration size and operation expense. To design a CPC collector, (1) the collector orientation, (2) two half acceptance angles θ_c, i.e. the original half acceptance angle and the truncated half acceptance angle, and (3) the optical gap g, viz. the distance between the CPC pinnacle and the base of the absorber, need to be determined according to the local meteorological conditions.

For practical applications, there are two possible orientations for the CPC. First of all, the CPC may be located in a vertical plane than contains the surface azimuth. This is termed the north-south placement. Alternatively, the CPC may be located in a transverse plane 90° from the longitudinal plane, viz. the east-west placement. Two issues are taken into consideration on determining the tube absorber orientation: one is to obtain the solar irradiation for at least 8 h per day, and the other is to guarantee a high concentration ratio. To the north-south placement, as the sun travels 15° on the sky per hour, it is obtained from Fig. 2 that $2\theta_c/15^\circ \geq 8$, viz. $\theta_c \geq 60^\circ$. The half acceptance angle is too large for the CPC to effectively concentrate the solar radiation, especially for the truncated CPC. To the east-west placement, the variation of the solar elevation angle is smaller than 0.5° in one day, which indicates that the annual variation of the solar elevation angles (also $2\theta_c$) is $23.45^\circ \times 2 = 46.9^\circ$. Its solar concentration ratio is much larger than the north-south orientated CPC's. This CPC can satisfy both considerations if laid on a tilted surface. It is also necessary that uniform flow to be maintained at all times in the tubular reactor, since non-uniform flows causes non-uniform residence times that can lower the efficiency compared to the ideal conditions. Correspondingly, the CPC with east-west orientation is more cost-effective and thus is applied in the present design.

The sunshine duration and solar irradiation in Xi'an, the location of the SKLMFPE, is presented in Table 2. It is shown from the table that the first three seasons take 80% of total sunshine duration and 85% of total solar irradiation in the year. Based on Table 2, an east-west orientated and north-south angle adjustable CPC is designed for the photoreactor. The half acceptance angle θ_c is 5°, with the maximum concentration ratio being 11.5. In order to reduce the material cost and decrease the configuration size, the CPC is truncated with the half acceptance angle being 60°. After truncation, the CPC concentration ratio is 4.12. As the local latitude of SKLMFPE is $\varphi = 34.25^\circ$, the adjustment range of the CPC titled angles would be $[\varphi\text{-}\delta, \varphi+\delta]$, viz., [10.8°, 57.7°]. According to the industrial standard in China, a DN25 Pyrex tube, whose inner diameter is 25.4 mm is selected as the absorber tube. The optical gap of the CPC is chosen as 25 mm from the engineering and construction points of view.

2.2. Design of a photoreactor module

A photoreactor with the designed CPC is then developed with a riser, a downcomer, a solution and gas inlet, a gas outlet and a condensing tube. Schematic of the proposed photoreactor unit operated under natural circulation is shown in Fig. 3 (a), and its

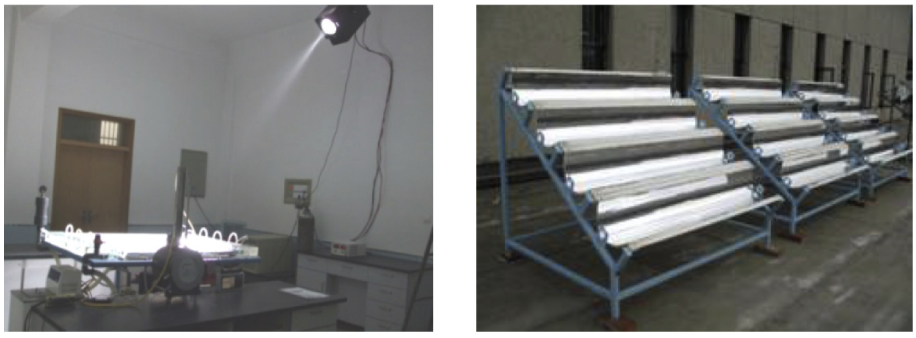

(a) (b)

Fig. 1. Reactors designed for photocatalytic hydrogen production at the SKLMFPE: (a) Generation 1, an indoor experimental setup; (b) Generation 2, an outdoor pilot-scale photoreactor with truncated CPCs.

Table 1
Parameters of two generations of photoreactor constructed at the SKLMFPE.

Generation	Site	CPC					Reactor		Photocatalyst (Concentration) Sacrificial agent (Concentration)	Hydrogen productivity
		Type	Orientation	Parameters			Area	Volume		
				θ_c/θ_d	d/g	C				
1	Indoor	Truncated	North-south	90°/90°	13.5/11.5	1	1	10	CdS (1 g L^{-1}) Na_2S/Na_2SO_3 (27.3 g L^{-1}/31.5 g L^{-1})	0.45 NL/h
2	Outdoor	Non-truncated	East-west	14°/30°	15/10	4.76	2.56	11.4	CdS (0.56 g L^{-1}) Na_2S/Na_2SO_3 (1.6 g L^{-1}/6.3 g L^{-1})	1.88 NL/h

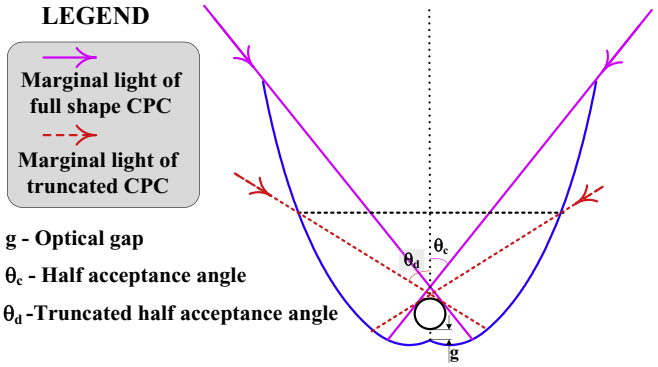

Fig. 2. Marginal light and major parameters of the CPC.

ideal T-s diagram is presented in Fig. 3 (b). As sunshine illumines the slurry solution in the absorber tube, the long-wave radiation causes its temperature rise and the shortwave radiation launches the photochemical reaction. Solar energy is transferred into the thermal and chemical energy by the manner of radiation and photocatalysis, causing the system entropy increase along the absorber tube. Then, the solution enters into the riser, along which the thermal energy of the solution partly changed into its gravitational potential energy as the system is constructed on the tilted surface. On the other hand, thermal energy loses to the surrounding by natural convection. The two processes both causes reduction of the system entropy. At the end of the riser, the generated hydrogen is drawn out of the photoreactor, causing a sudden drop of the entropy (*C*-*C*′) in Fig. 3 (b). After that, the slurry solution slows down and is cooled by natural convection along the horizontal condensing tube, thus the thermal energy of the solution losses to the surrounding. Correspondingly, the system entropy decreases along the condensing tube. Finally, the slurry flows back to the CPC through the downcomer, during which the gravitational potential energy transfers into the internal energy and the thermal energy losses to the surrounding through natural convection.

2.3. Two operation models

Slurry in the photoreactor is usually circled by pumps, which is one of the highest expends during the photocatalysis process. There are also some other situations, such as the first starting, overnight starting and long-term operation, under which the photocatalysts are fully sedimentary. Aiming to reduce the circulation energy consumption, a new operation strategy is proposed for the photocatalytic reactor: the natural circulation and gas disturbance combined model, viz. the photoreactor runs under the natural circulation model for most of the time, while the high pressure gas is filled in to perturb the sedimentary photocatalysts from time to time. The gas disturbance model is designed for these occasions: the high pressure gas, i.e. hydrogen or nitrogen, are filled into the photoreactor to disturb the sedimentary catalysts. Schematic of the two operation models is shown in Fig. 4. For the natural circulation model, the slurry solution is heated and illuminated along the CPC absorber tube, through which solution temperature rises and hydrogen bubble is generated. The large bubble section fraction and the high solution temperature cause the density difference between the absorber tube and the riser. Accordingly, the solution enters the riser under buoyancy effect. At the end of the riser tube, hydrogen bubble dissipates from the solution and is drawn out of the photoreactor. The solution is slowed down and cooled in the horizontal condensing tube. The low temperature solution finally flows back into the absorber tube through the downcomer under gravity effect. For the gas disturbance model, the high pressure gas, i.e. hydrogen or nitrogen, is filled into the photoreactor through the gas disturbance inlet. The high pressure gas flows in two ways before discharge from the reactor (see Fig. 4): one is along the path line of gas disturbance inlet - absorber tube - riser-gas outlet and the other is along the path line of gas disturbance inlet - downcomer - condensing tube - gas outlet. The turbulence generated by the high pressure gas can suspend the sedimentary photocatalysts effectively.

2.4. Supplementary components and photoreactor overview

3D schematic of the photoreactor is presented in Fig. 5. As shown in the figure, the CPC unit is fabricated from two highly reflective anodized aluminum CPC reflectors with 1.85 m-long absorber tubes. Six CPC units are connected in parallel by the riser, downcomer and the condensing tube, forming a complete module of photoreactors. The Pyrex glass tubes are connected by flanges and sealed by PTFE cushions. The frame support is made of galvanized steel pipes and its north-south movement around an east-west-oriented axis is available for roughly tracking the sun. East-west orientation is chosen with a small structural tilted angle (5°) in the same orientation as a way to make the solution flow smoothly along the channel. In addition, there are two inlets and three outlets in the reactor. Fresh solutions with high active photocatalysts and suited sacrifice agents are fed into the reactor through inlet 11 in Fig. 5. The high pressure gas is injected into the reactor for disturbance purpose through a low position inlet 2. The hydrogen generated by solar photocatalysis flows along the tubes,

Table 2
Sunshine duration and solar irradiation of each season in Xi'an.

Xi'an	Spring		Summer		Autumen		Winter		Annually
	Value	Percentage %	Value	Percentage %	Value	Percentage %	Value	Percentage %	Value
Sunshine duration (h)	480	24.3	643	32.5	461	23.3	393	19.9	1977
Total solar irradiation (kJ/cm^2)	120	26.2	163	35.8	102	22.4	71	15.6	456
Percentage of sunshine (%)	43		50		43		42		45

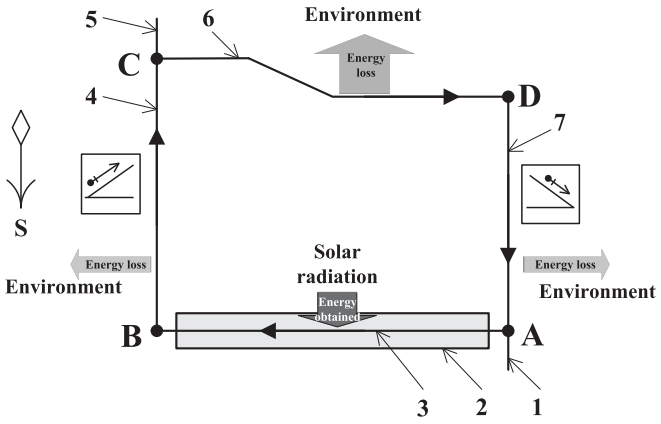

(a)

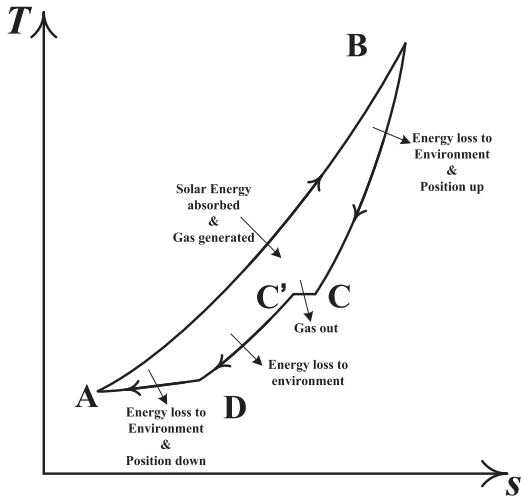

(b)

Fig. 3. Schematic of the solar photocatalytic reactor module: (a) the system flow chart and (b) the ideal T-s diagram of the natural circulation.

converges at the top of the collector and finally is drawn out of the reactor through the gas outlet 7. After a long-term running, the low activity photocatalysts and sacrifice agents are drained out of the reactor for post-processing through outlet 1. A special outlet 8 is reserved for the purpose of recovering the agglomerated photocatalysts and impurities.

3. Results and discussion

3.1. CPC performance

A Matlab program is developed to simulate the radiation distribution on the absorber tube surface by using Monte Carlo Method. Flowchart of the Matlab program is shown in Fig. 6. In the program, two groups of parameters, viz. control parameters and structural parameters, are input by the users according to the characteristics of the designed photoreactor. A coordinate system is established to describe the equations of the CPC and the absorber tube. The parallel light is launched with different incident angles toward the CPC. The light is then verified whether reaching the absorber tube top surface, the CPC surface or the tube bottom according to the line and curve equations in the coordinate system. And the determination of reflectance or absorbance is judged by comparing the reflectivity and the absorptivity to a random number generated by Matlab. Once the light is absorbed by the tube, its location is then recorded. Through this method, the radiation distribution on the absorber tube surface would finally be obtained. As the CPC half acceptance angle is 5°, three groups of critical lights, whose incoming angles are 5° left and right off and parallel to the central axis, are simulated and illustrated in Fig. 7 (a–i), (a–iii) and (a-ii) respectively. The light distribution on the absorber tube under these critical situations is presented in Fig. 7 (b). Because of the CPC's geometry, the light distribution under the conditions of Fig. 7 (a–i) and (a-iii) are asymmetrical. And shifting the incoming light off the central axis will decrease the maximum concentrated radiation and homogenize the radiation distribution on the absorber tube. In addition, simulation results also indicate that the light concentrating efficiency under the conditions of Fig. 7 (a–i), (a-ii) and (a-iii) are 65.8%, 71.6% and 65.4% respectively.

The monthly average total, CPC concentrated and absorbed irradiation together with the solar radiation and solar duration on different titled angles is shown in Fig. 8. It is easy to understand the curve of the total irradiation on horizontal. In addition, as the CPC is adjusted to roughly track the sun, the solar radiation on tilted surfaces is supposed to remain at a platform all through the year. On the other hand, the concentrated and absorbed solar irradiation both have the tendency of first increasing from January to June and then decreasing from June to December.

3.2. Slurry velocity under two operation models

3.2.1. Slurry velocity under the natural circulation

In the natural circulation model, slurry density is a function of the temperature and section void fraction (SVF), which could be expressed as:

$$\rho = \rho(T, SVF) \tag{1}$$

The SVF is defined as:

$$SVF = \frac{V_{H2}}{V_{H2} + \pi r^2 v_{mix}} \tag{2}$$

where V_{H2} is the hydrogen productivity in the reactor, r is the tube radius and v_{mix} is the slurry velocity.

For the multiphase flow in the tube, the slurry density is determined by the volume ratios of the solution and the gas, which could be expressed as:

$$\rho_{mix} = \rho_l(T)(1 - SVF) + \rho_g(T)SVF \tag{3}$$

The density difference between the riser and the absorber tube is:

$$\Delta\rho = \rho_l(T) - \rho_{mix}(T) \tag{4}$$

Taking Eq. (3) into Eq. (4), it is obtained that

$$\Delta\rho = \rho_l(T)SVF - \rho_g(T)SVF \tag{5}$$

The continuity equation in the reactor is:

$$\rho_l(T)v_{l,7}A_7 = \sum_{i=1}^{6} \rho_{mix,i}v_{mix,i}A_i \tag{6}$$

where $v_{mix,i}$ is the mixture velocity in the ith absorber tube, $v_{l,7}$ is the solution velocity in the end of the riser (see Fig. 4) and A is the tube section area.

The energy equation in the CPC is:

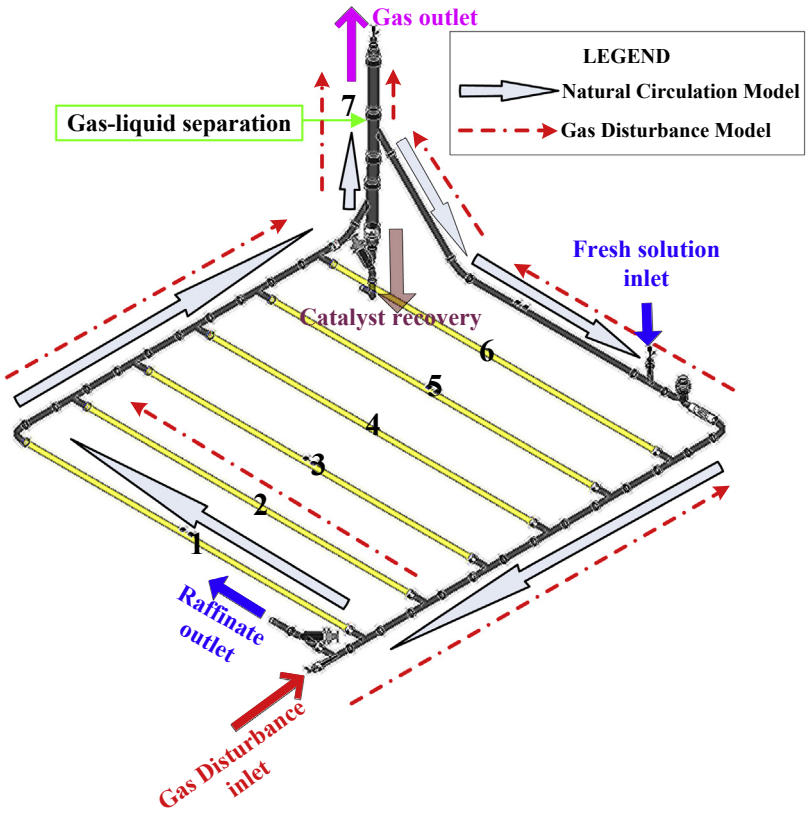

Fig. 4. Schematic of the two operation models in the photoreactor.

$$Q = c_p \rho_{mix,i} A_i v_{mix,i} \Delta T \tag{7}$$

The momentum equation in the reactor is:

$$\rho_{mix,i}\left(\lambda \frac{l}{d} + \zeta\right)\frac{v_{mix,i}^2}{2} = \Delta p_i \tag{8}$$

where λ and ζ are frictional and local resistance loss coefficients and Δp_i is the pressure between the absorber tube and the riser in the ith absorber tube, which can be calculated according to the next equation:

$$\Delta p_i = \Delta \rho_i g h_i \tag{9}$$

where h_i is the altitude difference between the absorber tube and the end of the ith riser and $\Delta \rho_i$ is the density difference between the ith absorber tube and the riser (see Fig. 4).

For the laminar flow, the frictional loss coefficient is

$$\lambda = \frac{64}{\mathrm{Re}} = \frac{64\mu}{\rho_{mix} v_{mix} d} \tag{10}$$

The slurry velocities in the absorber tube and the slurry temperature could be confirmed through simultaneous Eqs. (6)–(8). In this study, the photocatalyst is $Cd_{0.5}Zn_{0.5}S$ (1 g/L) and the sacrifice agents are Na_2S and Na_2SO_3 (both 0.25 mol/L). The photocatalyst "$Cd_{0.5}Zn_{0.5}S$" has special nano-twin-crystal structure, and can be formed with the phase interface. This kind of structure can promote the separation of electrons and holes effectively and obtain high activity of hydrogen production. It can also be scaled up for mass production, without noticeable decrease of the activity. Lab-scale experiments indicate that the photocatalyst ($Cd_{0.5}Zn_{0.5}S$) could stay activity at a high level for 72 h. Detailed characteristics of the photocatalyst can be found in Ref. [3]. The slurry density and velocity in each tube are finally obtained and presented in Fig. 9. It is found from the figure that both the slurry velocities and densities decline gradually from the base to the top. This is resulted from the decreasing altitude differences between the absorber (from tube No. 1 to No. 6) and the riser.

3.2.2. Gas disturbance critical velocity

With respect to the gas disturbance velocity, a limiting settling velocity (V_{LS}) is adopted to estimate the slurry status, and is defined as the critical velocity in a horizontal pipeline, below which photocatalysts begin to settle along the tubes. Though there are many empirical equations proposed to determine the limiting settling velocity for heterogeneous slurry in a horizontal tube [12–15], few equations are suitable for this study as the photocatalyst diameter is in the level of tens of micrometers. Even if the photocatalysts are agglomerated, the maximum diameter is as large as 70–80 μm. According to the applicable scope, three equations proposed by Wasp [13], Кроюз [14] and Wang [15] are found to be suitable for the present study.

Durand proposed a well-accepted equation for calculating the critical flow velocity [12]. However, Durand's equation is not suitable for particle diameter $d < 0.5$ mm. Wasp revised Durand's equation by adapting into the influence of the particle diameter. The equation proposed by Durand and Wasp are [12,13]:

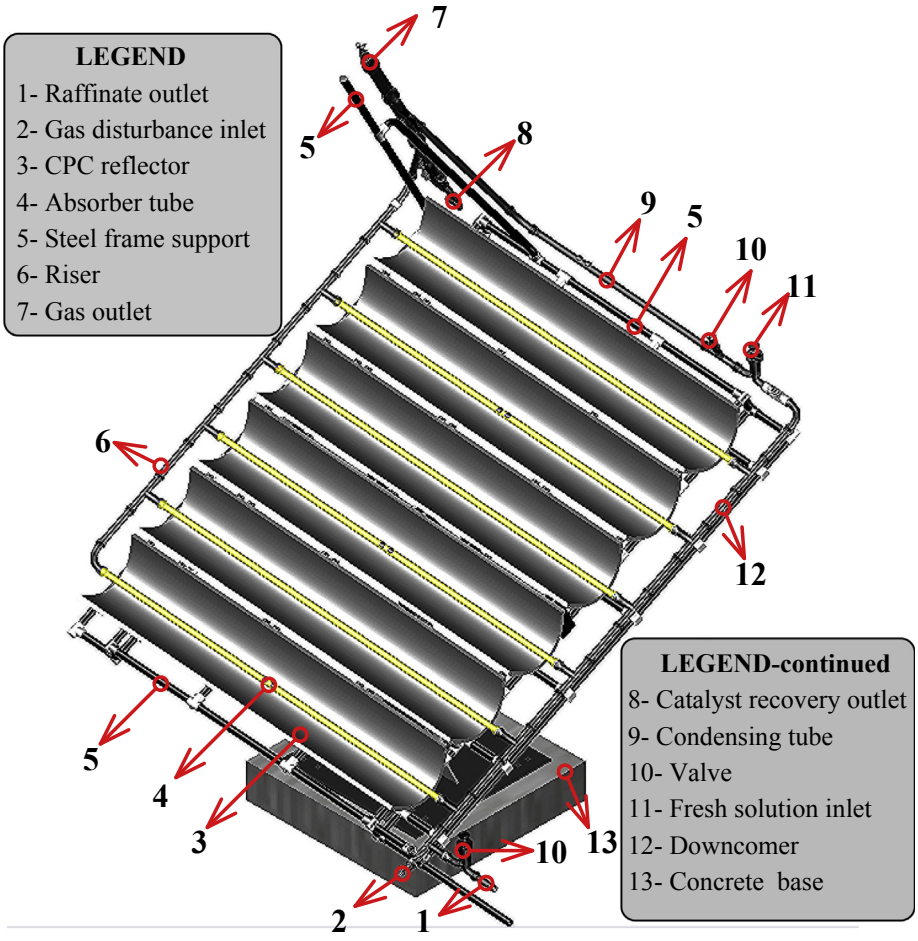

Fig. 5. 3D schematic of the designed photoreactor.

Durand Equation:

$$V_{LS} = F_L\left[2gD\left(\frac{\rho_s - \rho_l}{\rho_l}\right)\right]^{\frac{1}{2}} \tag{11}$$

Wasp Equation:

$$V_{LS} = F_L'\left[2gD\left(\frac{\rho_s - \rho_l}{\rho_l}\right)\right]^{\frac{1}{2}}\left(\frac{d_s}{D}\right)^{\frac{1}{6}} \tag{12}$$

where ρ_s and d_s are the particle density and diameter respectively, D is the tube diameter, F_L and F_L' are the coefficients determined by the particle diameter and volume concentration.

Кроюз proposed a series of empirical equations suitable for different particle diameters in horizontal tubes [14], and for $d_s \leq 0.07$ mm the equation is:

$$V_{LS} = 0.2 \times \left(1 + 3.43 \times \sqrt[4]{\frac{100 c_W}{1 - c_W} d_s^{0.75}}\right) \frac{s - 1}{1.7} \tag{13}$$

where c_W and s are the specific gravity and mass concentration of the photocatalyst.

Wang et al. proposed an empirical equation according to the energy balance in the multiphase flow [15], in which they introduced the weighted average hydraulic coarseness $\bar{w}$ to illustrate the influence of the particle concentration and w_{95}/w to reflect the inhomogeneity of particles. Their equation is expressed as:

$$V_{LS} = 3.72 d_s\left[\left(\frac{s_m - 1}{s_m}\right)(1 - C_V)^n \bar{w}\right]^{0.25}\left(\frac{w_{95}}{\bar{w}}\right)^{0.2} \tag{14}$$

where s_m is the slurry specific gravity, C_V is the particle volume concentration and

$$w = \frac{d^2(\rho_s - \rho_l)g}{18\mu} \tag{15}$$

$$n = 5 - \log \mathrm{Re}_d \tag{16}$$

where $\mathrm{Re_d}$ is the particle Re number, and can be calculated by:

$$\frac{\mathrm{Re}_d = d_s \bar{w}}{\nu_w} \tag{17}$$

The limiting settling velocities calculated according to Eqs. (12)–(14) under different catalyst diameters are shown in Fig. 10. As these equations are obtained through different experimental researches, calculated results of these equations are not exactly anastomotic. Eqs. (12) and (14) predict similar limiting settling velocity for photocatalysts diameters below 10 μm. In general, Fig. 10 indicates that in order to perturb the photocatalysts in the horizontal absorber, the slurry velocity should be over 1 m/s. Comparing Figs. 9 and 10, it is found that the slurry velocity under the natural circulation conditions is much smaller than the limiting settling velocity, which validates necessity of the gas disturbance.

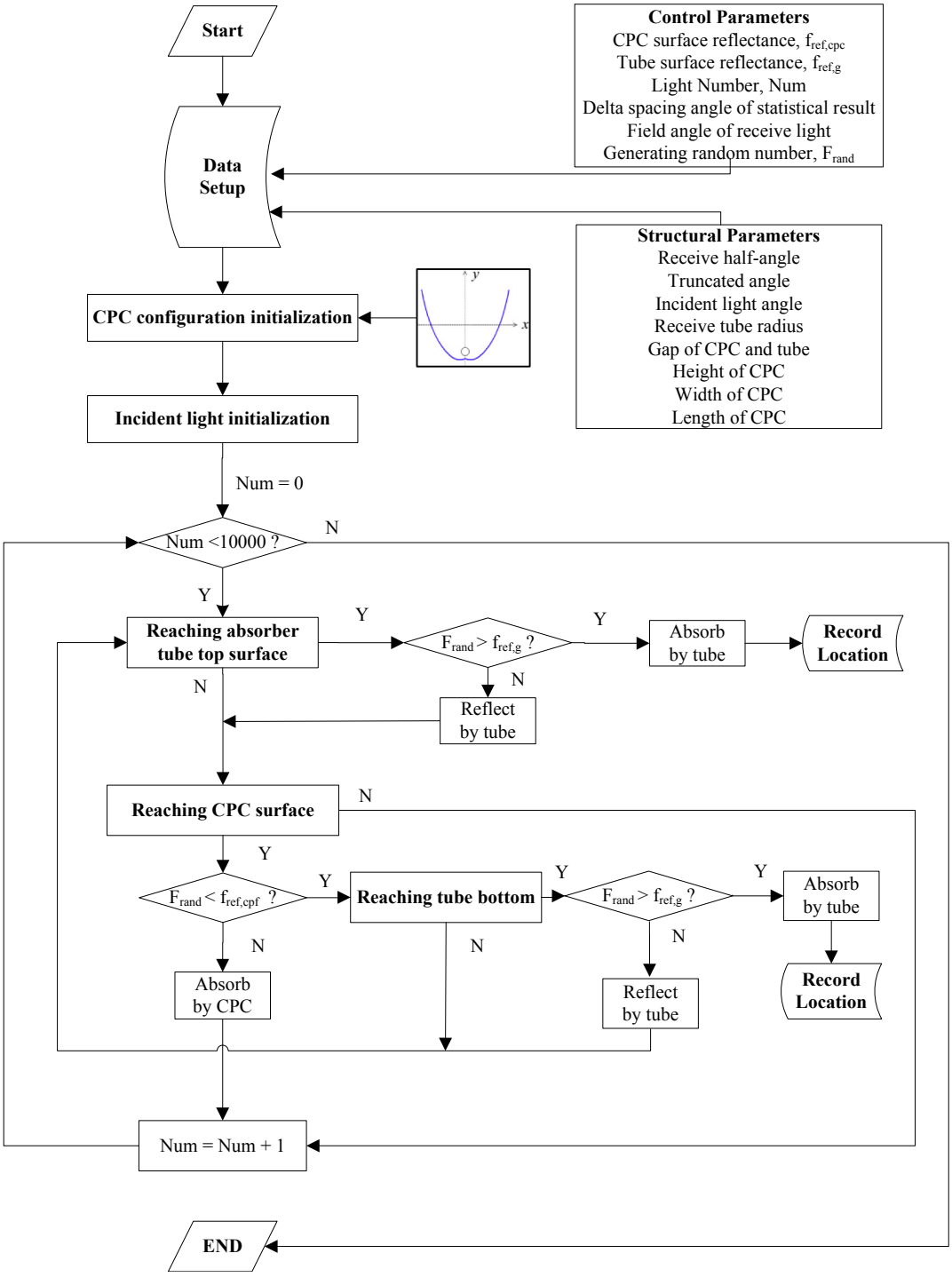

Fig. 6. Flowchart to simulate the radiation distribution on the absorber tube surface by using Monte Carlo Method and Matlab program.

Also the limiting settling velocity guides the pressure and flow rates of the injected high pressure gas.

3.3. Hydrogen productivity prediction

The interpolation energy conversion efficiencies of $Cd_{0.5}Zn_{0.5}S$ under different solar radiation wavelengths are shown in Fig. 11 [16]. The energy distribution of the solar radiation under different wavebands with different CPC tilted angles is presented in Table 3. According to Fig. 11 and Table 3, the ideal hydrogen production during two typical weeks in spring and summer (including the spring equinox and the summer solstice respectively) is shown in Fig. 12. From the figure, it is found that the hydrogen production is highly relevant to the solar irradiation and that it is daily periodic in the summer week but daily fluctuant in the spring week. The highest ideal hydrogen productivities in the summer week steadily remain near 4.5 L/h whereas the highest ideal hydrogen productivities in the spring week are variable in the range of [1.34 L/h, 5.26 L/h]. Statistical results from Fig. 12 indicate that the mean ideal hydrogen productivities are 2.9 L/h and 20.5 L/day in the spring

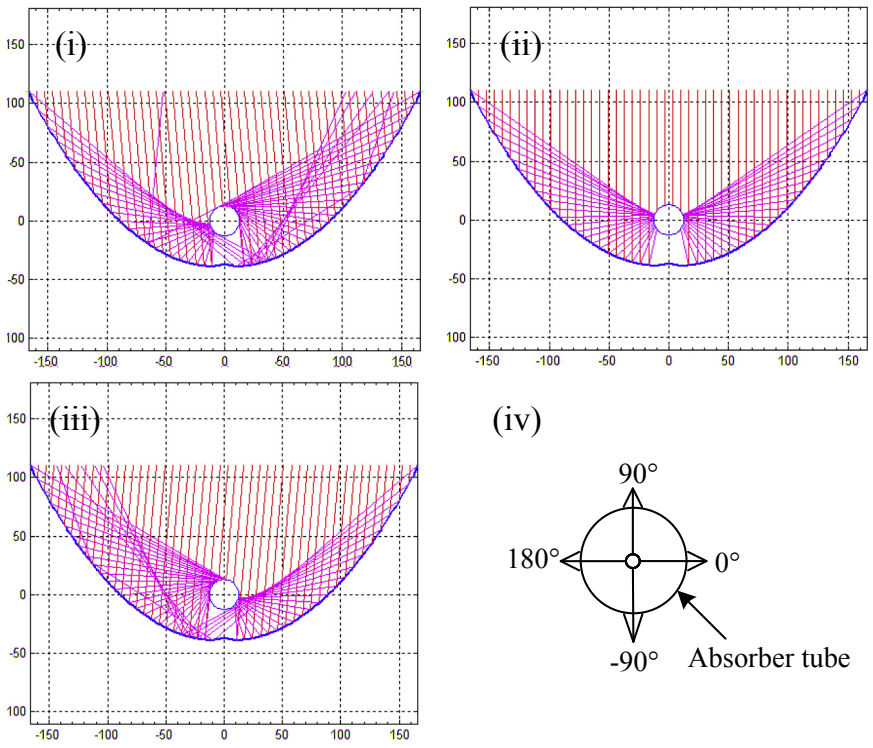

(a)

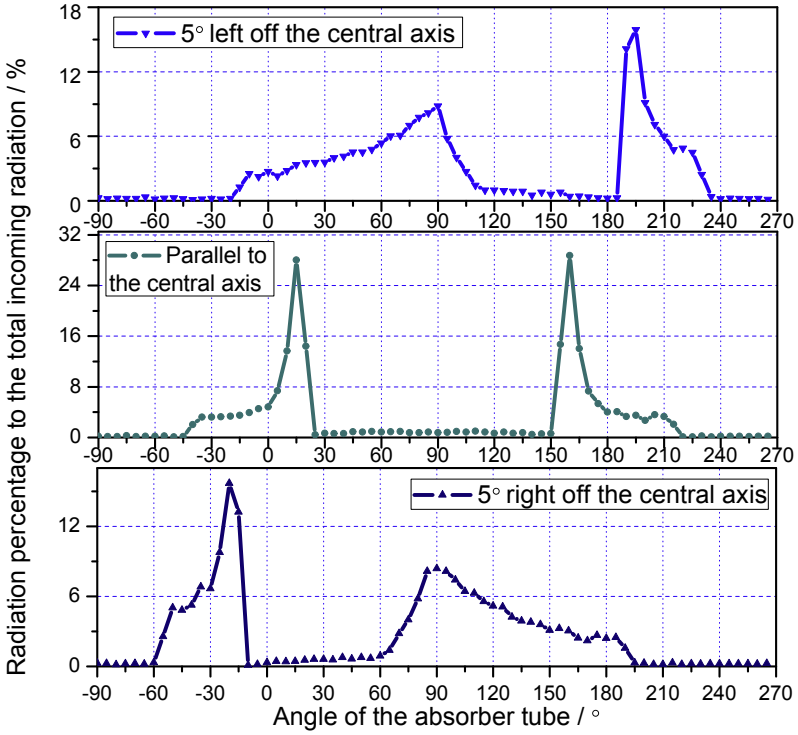

(b)

Fig. 7. (a) Ray tracing of incoming light for the CPC when: (i) incident angle is 85°, (ii) incident angle is 90° and (iii) incident angle is 95°; (b) Incoming light distribution on the absorber tube surface with incoming incident angle being 85°, 90° and 95° respectively.

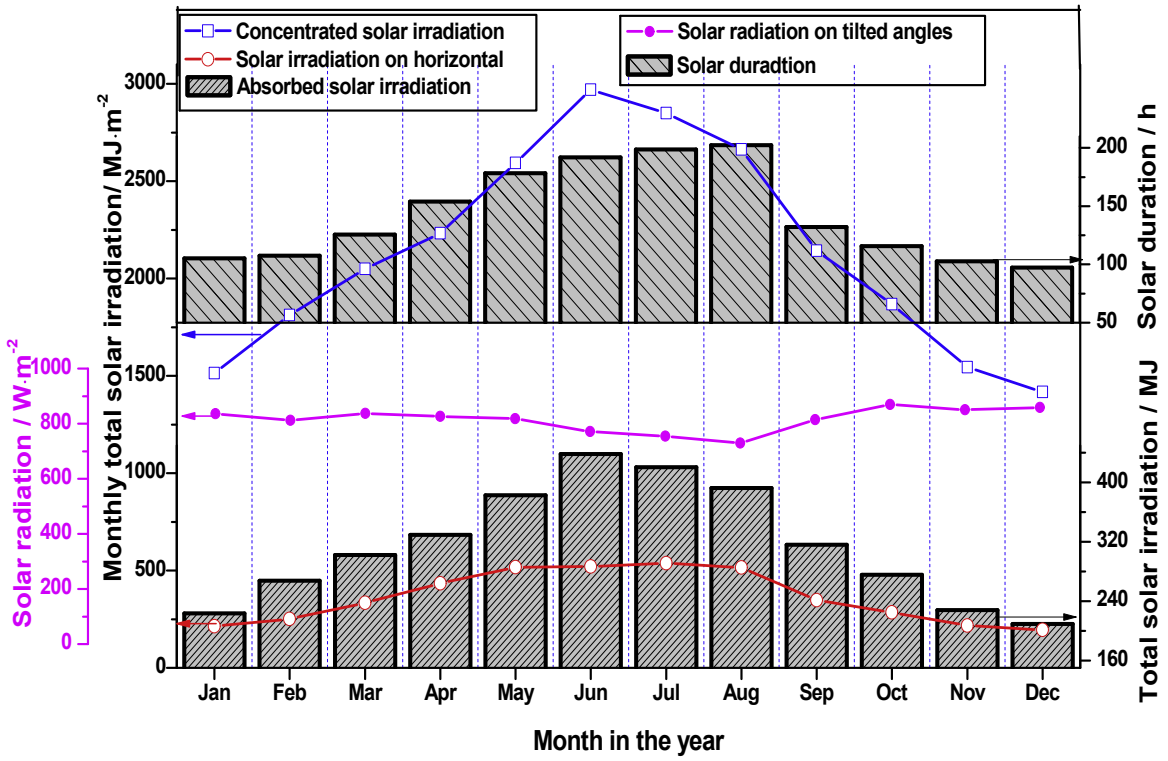

Fig. 8. Monthly average total, CPC concentrated and tube absorbed solar radiation and duration on different tilted angles in the year.

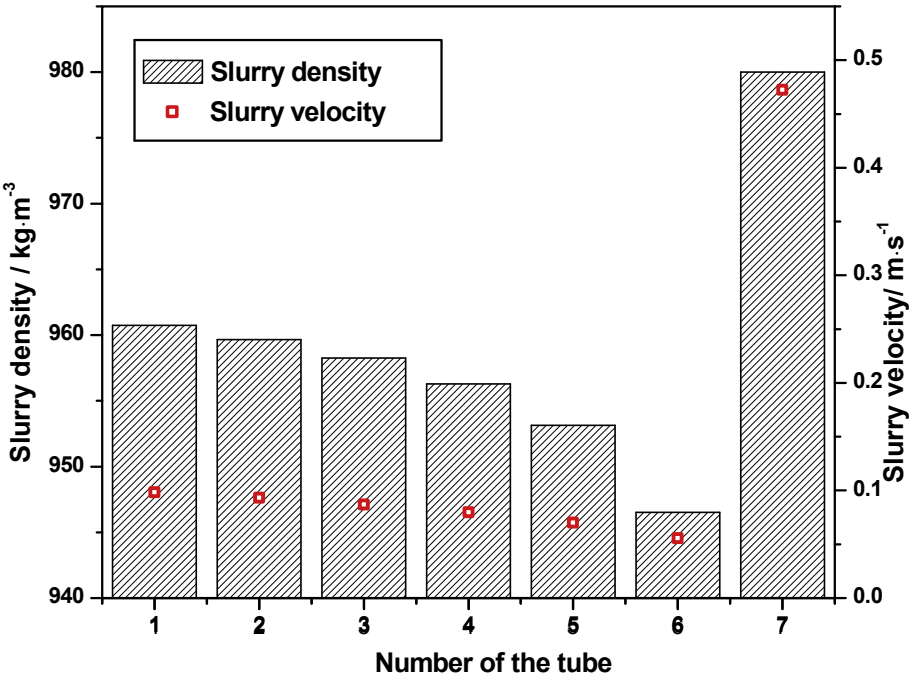

Fig. 9. Slurry density and velocity in each tube ($\zeta = 34$, $\mu = 0.5 \times 10^{-3}$ Pa s, $V_{H2} = 1$ mL/s).

week, and 4.0 L/h and 36.1 L/day daily in the summer week.

4. Conclusions

In this study, a CPC photoreactor is designed according to the meteorological conditions at the SKLMFPE. Two operation models, i.e. the natural circulation model and the gas disturbance model, are proposed for the purpose of reducing the energy consumption during the photocatalysis process. The photoreactor performances, viz. the CPC light distribution, the slurry critical velocities and the

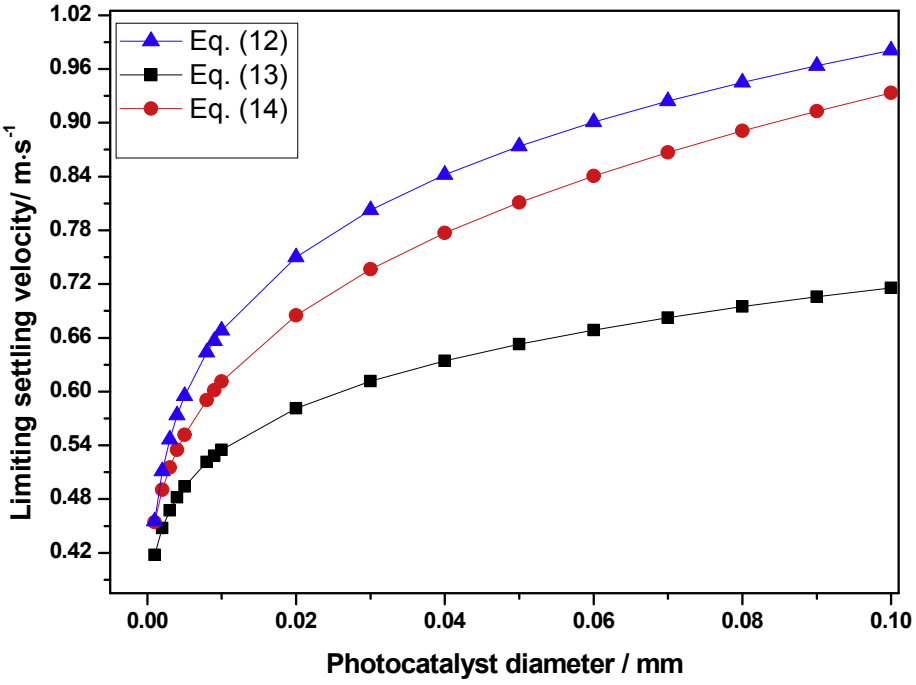

Fig. 10. Critical settling velocities in the horizontal tube of the photoreactor under different catalyst diameters.

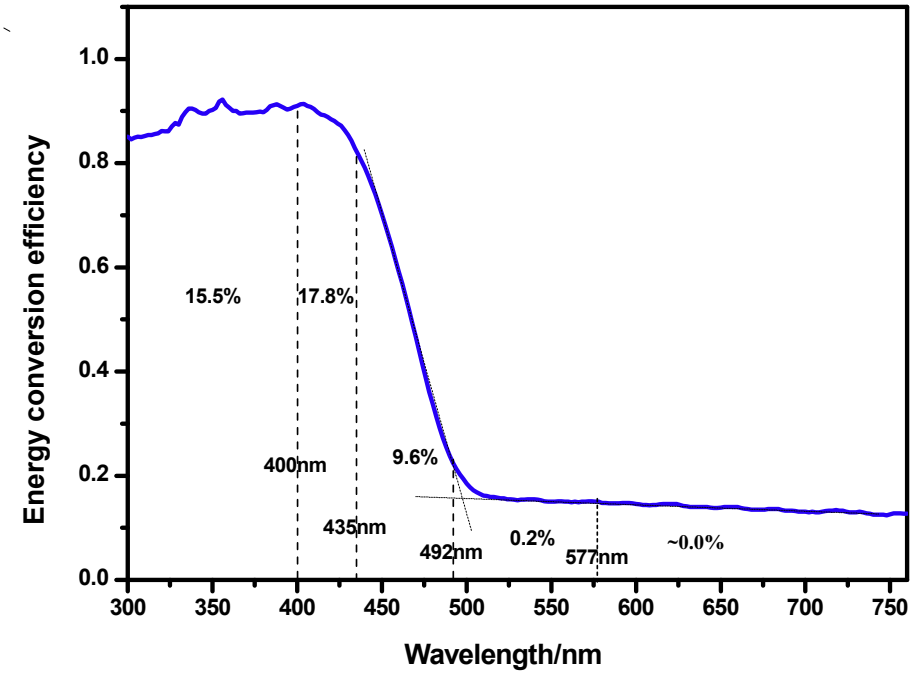

Fig. 11. Energy conversion efficiency of $Cd_{0.5}Zn_{0.5}S$ under different solar radiation wavelengths.

photocatalytic hydrogen productivity are estimated and discussed. Six north-south orientated, angle monthly adjustable and truncated CPCs are connected in parallel with a riser, a downcomer and a condensing tube, forming a natural circulated photoreactor. The natural circulation velocities in the photoreactor are diminishing from the base tube to the top tube and are below 0.1 m/s. On the other hand, the required limiting settling velocity for disturbance is 1 m/s. The average ideal hydrogen production productivities in a typical summer week are 4.0 L/h and 36.1 L/day, and in a typical spring week are 2.9 L/h and 20.5 L/day. The exciting results promote the authors to construct, install and scale up the designed reactor for a pilot demonstration of direct solar photocatalytic hydrogen production.

Table 3
Energy distribution of the solar radiation under different waveband with different CPC tilted angles.

CPC angle (°)	Infrared light (%)	Visible light (%)						Ultraviolet light(%)
	>760 nm	760 nm~622 nm	622 nm~577 nm	577 nm~492 nm	492 nm~435 nm	435 nm~400 nm	760 nm~400 nm	300 nm–400 nm
10.8	50.28	12.16	10.02	9.27	8.83	5.04	45.32	4.40
18.6	50.60	12.13	10.03	9.22	8.74	4.99	45.11	4.30
26.4	50.70	12.16	10.08	9.20	8.66	4.95	45.04	4.26
34.2	50.88	12.22	10.11	9.17	8.55	4.87	44.93	4.20
42.0	51.23	12.35	10.10	9.11	8.39	4.75	44.70	4.08
49.8	52.10	12.55	9.97	8.97	8.11	4.51	44.12	3.78
57.7	53.50	13.02	9.68	8.73	7.67	4.10	43.20	3.30

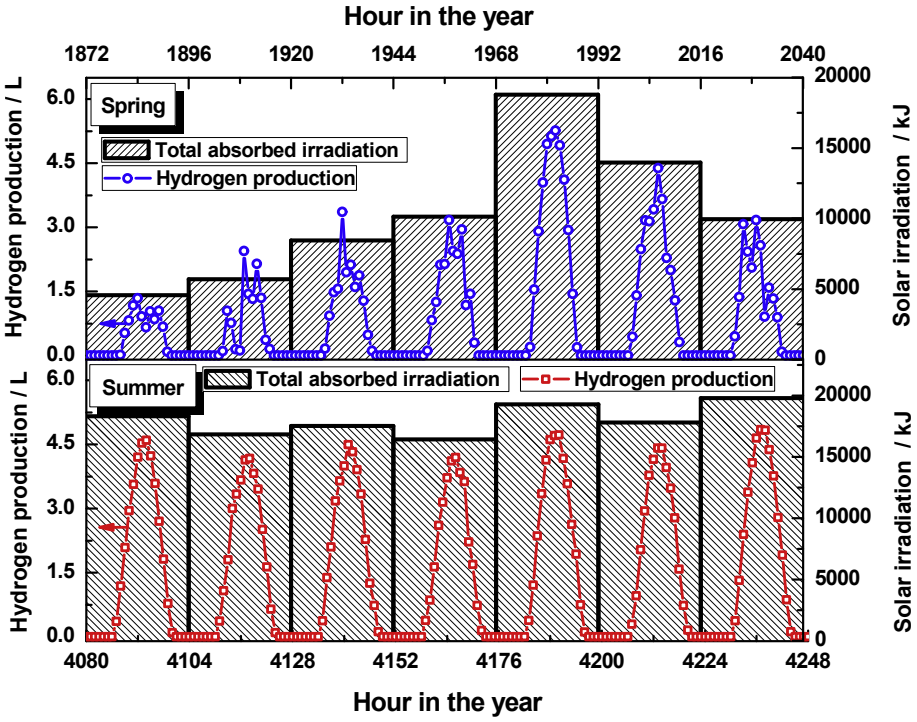

Fig. 12. Hydrogen productivity and total absorbed solar irradiation during two typical weeks in spring and summer.

Acknowledgements

This research was funded by the National Natural Science Foundation of China (No.: 51506043), the National High Technology Research and Development Program of China (863 Program, No.: 2012AA051501), the US National Science Foundation Support (Grant No.: CMMI-1351817), the China Scholarship Council (Grant No.: 201706715058) and the "Dayu Scholar" foundation of Hohai University.

References

[1] A.A. Ismail, D.W. Bahnemann, Photochemical splitting of water for hydrogen production by photocatalysis: a review, Sol. Energy Mater. Sol. Cells 128 (128) (2014) 85–101.
[2] H. Ahmad, S.K. Kamarudin, L.J. Minggu, et al., Hydrogen from photo-catalytic water splitting process: a review, Renew. Sustain. Energy Rev. 43 (2015) 599–610.
[3] M. Liu, L. Wang, G. Lu, et al., Twins in Cd1−xZnxS solid solution: highly efficient photocatalyst for hydrogen generation from water, Energy & Environ. Sci. 19 (4) (2011) 1372–1378.
[4] C. Minero, E. Pelizzetti, S. Malato, et al., Large solar plant photocatalytic water decontamination: degradation of pentachlorophenol, Chemosphere 26 (12) (1993) 2103–2119.
[5] W. Gernjak, M.I. Maldonado, S. Malato, et al., Pilot-plant treatment of olive mill wastewater (OMW) by solar TiO2, photocatalysis and solar photo-Fenton, Sol. Energy 77 (5) (2004) 567–572.
[6] S. Malato, J. Blanco, A. Vidal, et al., Photocatalysis with solar energy at a pilot-plant scale: an overview, Appl. Catal. B Environ. 37 (1) (2002) 1–15.
[7] S. Malato, J. Blanco, C. Richter, et al., Low-concentrating CPC collectors for 11 photocatalytic water detoxification: comparison with a medium concentrating solar collector, Water Sci. Technol. 35 (4) (1997) 157–164.
[8] J. Blanco, S. Malato, P. Fernandez, A. Vidal, A. Morales, P. Trincado, et al., Compound parabolic concentrator technology development to commercial solar detoxification applications, Sol. Energy 67 (1999) 317–330.
[9] A. Vidal, A.I. Diaz, A.E. Hraiki, et al., Solar photocatalysis for detoxification and disinfection of contaminated water: pilot plant studies, Catal. Today 54 (2) (1999) 283–290.
[10] M.C. Liu, D.W. Jing, L. Zhao, L.J. Guo, Preparation of novel CdS-incorporated special glass composite as photocatalyst material used for catalyst-fixed system, Int. J. Hydrogen Energy 35 (2010) 7058–7064.
[11] D. Jing, H. Liu, X. Zhang, et al., Photocatalytic hydrogen production under direct solar light in a CPC based solar reactor: reactor design and preliminary results, Energy Convers. Manag. 50 (12) (2009) 2919–2926.
[12] R. Durand, The Hydraulic Transportation of Coal and Other Materials in Pipes, College of National Coal Board, London, 1952.
[13] E.J. Wasp, J.P. Kenny, B.L. Gandhi, Solid-liquid Flow Slurry Pipeline Transportation, Clausthal: Trans. Tech. Publications, 1977.
[14] B.C. Кроюз, Design of Concentrator Tailings Facilities, Metallurgical Industry Press, Beijing, 1959 (in Chinese).
[15] S.Z. Wang, W.C. Wang, P. Sun, Granular Material Slurry Pipeline Transport, Ocean Press, Beijing, 1998 (in Chinese).
[16] Y.J. Zhang, L.J. Guo, W. Yan, L. Zhao, H.H. Yang, M.T. Li, Y.B. Xu, Experimental and calculation of energy conversion efficiency and quantum yield in the system of hydrogen photoproduciton by water splitting, Acta Energiae Sol. Sin. 27 (11) (2006) 1113–1116 (in Chinese).